A Novel Superconducting MRI Magnet and Its Optimum Design Using Adaptive Optimization Strategy

Yanli Zhang, Yangyang Wang, Wenyue Huang, Dexin Xie, Baodong Bai
Department of Electrical Engineering, Shenyang University of Technology, China
E-mail: zhangyanli_sy@hotmail.com

***Abstract*—This paper proposes an open superconducting magnetic resonance imaging (MRI) magnet configuration with the addition of soft magnetic material. In order to obtain multiple optimization design objectives including high homogeneity in the imaging region, high magnetic field strength as well as low cost, a two-step optimization strategies are carried out, in which orthogonal design (OD) is, firstly, employed to define the key ones among several possible design variables and then response surface model (RSM) with high computation efficiency is utilized to simulate the objective function. The magnetic performance in the imaging region of MRI attains to the design requirement.**

***Index Terms*—Magnetic resonance imaging, Optimization methods, Response surface methodology, Superconducting magnets.**

I. INTRODUCTION

For traditional superconducting MRI system, the imaging region is completely enclosed by the solenoid coil, and this may induce claustrophobia to some patients and make interventional diagnostic or surgical procedures difficult. However, open accessibility to the imaging region may cause the less energy efficiency of the magnets and worse magnetic field homogeneity [1-3]. In this paper, a novel magnet structure of open-type superconducting MRI device composed of iron material and superconducting coil is presented. Owing to the addition of soft magnetic material to superconducting magnet, the main magnetic circuit excited by superconducting coils can be closed through iron and air region so that the openness of imaging region increases. The magnetic field in the imaging region is obtained with the 3-D finite element analysis (FEA). The orthogonal design (OD) and an adaptive optimization strategy using response surface model (RSM) are proposed to obtain the optimal design of MRI with higher magnetic efficiency as well as higher degree of access to imaging region.

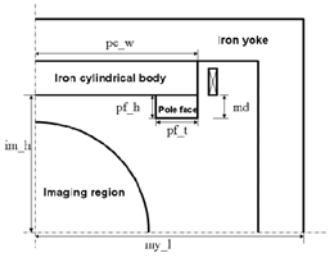

Fig. 1. The open-type superconducting MRI magnet.

TABLE I
EFFECTS OF FIELD INHOMOGENEITY FROM 6 DESIGN VARIABLES

Design variables	*my_l*	*pc_w*	*im_h*	*md*	*pf_t*	*pf_h*
$\Delta\delta(\times 10^{-4})$	2	33	7	6	63	48

II. OPTIMIZATION COURSE

A. The determination of key design variables

An initial model of the open-type superconducting MRI magnet is shown in Fig. 1, in which a couple of superconducting coils are winded outside cylindrical body made from ferromagnetic material. The magnetic field in the imaging volume which is a spherical space with a diameter of 40cm is generated by the superconducting coils. There are 6 design variables (DVs) to define magnet configuration, i.e. *my_l*, *pc_w*, *im_h*, *md*, *pf_t* and *pf_h* shown in Fig. 1, and the orthogonal design (OD) is developed to find out the key design variables among them. In this paper, Taguchi's orthogonal table is used to calculate the variation trend of magnetic flux density and non-homogeneity in the imaging region with all variables mentioned above. The results listed in Table I show that these six design variables within their own scopes always guarantee that the magnetic flux density attains to above 1.5T, but the interaction between the two variables *pf_t* and *pf_h* have greater effect on the inhomogeneity .

Thus, the size of *pf_t* and *pf_h* of the pole face shape are defined as key design variables and *pc_w*, *my_l*, *im_h* and *md* are fixed at 0.63m, 1.37m, 0.28m and 0.01m, respectively. The optimization objective is defined as follows:

$$F(\vec{x}) = \frac{\delta}{\delta_{norm}} + \frac{|B_{ave} - B_{norm}|}{B_{norm}} \tag{1}$$

where B_{ave} is the mean value of the magnetic flux densities, δ is the non-homogeneity in the imaging region, and $\vec{x} = (pf\_t, pf\_h)$ with the scope of $pf\_t \in [0.25, 0.35]\text{m}$, $pf\_h \in [0.01, 0.04]\text{m}$. δ_{norm} and B_{norm} are allowed field value in intensity and non-homogeneity, and are set as 300ppm and 1.5T, respectively.

B. Adaptive Optimization Strategy

In order to reduce the computational work related with 3-D

finite element analysis during the optimal design, an adaptive optimization strategy is suggested by successive reduction of the design space and adaptive inserting of new sampling points. The response surface model (RSM) using multi-quadric radial basis function [4] is to approximate the objective function. Once a response surface has been constructed, a minimum point can be easily found by applying (1+ λ) evolution strategy. The minimum point obtained at this stage, however, can not be considered as a true optimal point unless sufficient number of sampling data is involved in the construction of the response surface. This minimum point hereinafter will be referred to a *pseudo-optimal* point. The proposed optimization algorithm using adaptive response surface method can be summarized as follows:

Step 1 Define the initial design space, and generate uniformly distributed N_i Pareto-optimal sampling points in the whole design space by means of Latin hypercube design with *Max Distance* and *Min Distance* criteria.

Step 2 Construct a response surface using multi-quadric radial basis function, and find a *pseudo-optimal* point by applying (1+λ) evolution strategy.

Step 3 Check the convergence of the *pseudo-optimal* points, and stop if converged.

Step 4 Reduce the design space by a suitable factor with the center of the current pseudo-optimal point.

Step 5 Generate additional N_a Pareto-optimal sampling points only within the reduced design space concentrating at the neighborhood of the current *pseudo-optimal* point as in *Step 1*, and go to *Step 2*.

In the algorithm, the iteration repeats until the *pseudo-optimal* points converge, and the converged *pseudo-optimal* point is considered as a true optimal point. The proposed algorithm is applied to TEAM problem 22 [5], and its robustness and computational efficiency are investigated. Table II compares the performance of the proposed method with those of the other reported solutions. The best solution for this problem is reported in [5] as listed in Table II.

III. Optimum Design

By utilizing proposed optimization algorithm, the magnet in Fig.1 is optimized. During the optimization procedure, the initial 25 Pareto-optimal sampling points are distributed in the whole design space, and followed by successive additional insertion of 16 and 11 sampling points into the reduced design space with a factor of 0.618 to the previous region. After 3 iterations, a converged optimal point are obtained and the constructed response surface of objective function is shown in Fig.2 and the comparison results between before and after optimization are listed Table III. The magnetic flux density distribution in the imaging region is shown in Fig.3. Through the optimal design, the suggested superconducting magnet configuration is proven to provide an enough homogeneous and sufficiently strong magnetic fields for MRI application.

TABLE II
COMPARISON OF DIFFERENT ALGORITHMS

Algorithm	R_2	$h_2/2$	d_2	objective function	No. of FEM computations
Proposed	3.093	0.239	0.391	0.0895	180
GA	3.05	0.246	0.400	0.122	2400
TEAM[5]	3.08	0.239	0.394	0.088	-

References

[1] J. H. Bae, K. D. Sim, R. K. Ko, et al, "The fabrication of superconducting magnet for MRI," *Phy. C*, vol. 372-376, Part 3, pp. 1342-1345, August 2002.

[2] V. Vegh, Q. M. Tieng, I. M. Brereton, "Minimum stored energy MRI superconducting magnets: from low to high Field," *Concepts in Magnetic Resonance Part B* (Magnetic Resonance Engineering), vol. 35B(3), pp. 180–189, June 2009.

[3] Q. M. Tieng, V. Vegh, I. M. Brereton, "Minimum stored energy high field MRI superconducting magnets," *IEEE Transactions on Applied Superconductivity*, vol.19, no.4, pp. 3645-3652, August 2009.

[4] S. Rippa, "An algorithm for selecting a good value for the parameter c in radial basis function interpolation," *Advances in Computational Mathematics*, Vol. 11, pp. 193-210, 1999.

[5] B. Brandstaetter, "SMES optimization benchmark, TEAM Problem 22, 3 parameter problem," http://www.igte.tu-graz.ac.at/archive/team_new/team3.php.

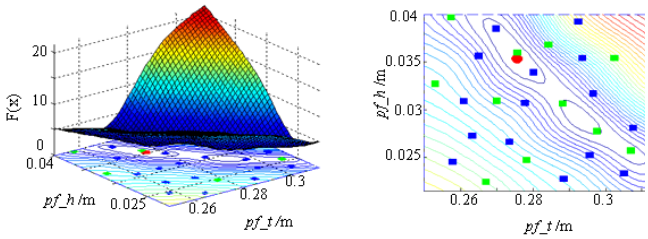

Fig.2 The sampling points distribution and corresponding response surface at the third iteration of adaptive optimization course.

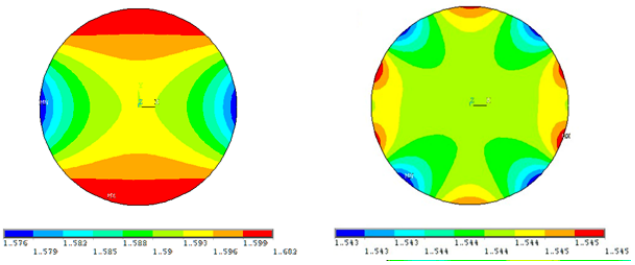

(a) before optimization (b) after optimization

Fig.3 The distribution of magnetic flux density in the imaging region before and after optimization.

TABLE III
COMPARISON OF COMPUTATION RESULTS BEFORE AND AFTER OPTIMIZATION

	pf_t (mm)	*pf_h* (mm)	*B* (T)	δ (ppm)
before optimization	250	10	1.55	60.9
after optimization	276	36	1.54	2.6